Gerardo Marx Chávez-Campos
Professor at Tecnológico,
Nacional de México/IT Morelia,
1500 Av. Tecnológico, Morelia,
Michoacán, 58120 México
e-mail: gmarx_cc@itmorelia.edu.mx

Adriana del Carmen Téllez-Anguiano
Professor at Tecnológico,
Nacional de México/IT Morelia,
1500 Av. Tecnológico, Morelia,
Michoacán, 58120 México
e-mail: adrianat@itmorelia.edu.mx

Juan Alfonso Salazar-Torres
Professor at Tecnológico,
Nacional de México/IT Morelia,
1500 Av. Tecnológico, Morelia,
Michoacán, 58120 México
e-mail: jast2007@hotmail.com

Héctor Javier Vergara-Hernández
Professor at Tecnológico,Nacional de México/IT Morelia,
1500 Av. Tecnológico, Morelia,
Michoacán, 58120 México
e-mail: hvergarah@yahoo.com

Octavio Vazquez-Gómez
Professor at Tecnológico,
Nacional de México/IT Morelia,
1500 Av. Tecnológico, Morelia,
Michoacán, 58120 México
e-mail: aanubbis@hotmail.com

An Ohmic Heating Model Based on the Thermal Circuit Method: Case of Study for Parameter Determination

Currently, ohmic heating is a method with a wide potential as an alternative thermal process in the industry. However, the success of this method depends on the rate of the generated heat by the right material's selection and its geometry. Due to its complexity, the heating systems are usually modeled by computational fluid dynamics (CFD) or finite element method (FEM). However, in this paper, an alternative model representation was used, and this model does not consider the temperature gradients and uses thermal resistance and capacitance as steady-state and transient analog parameters. The parameters are calculated using MATLAB *considering the geometry, as well as the electrical and thermal properties of the material to heat. The proposed circuit is solved by applying the Laplace transform. Finally, the temperature performance of the model and the experimental system are compared with noncontrolled and controlled experiments.*
[DOI: 10.1115/1.4043897]

1 Introduction

A heat treatment is a method used to improve the mechanical or chemical properties of a product in several industries such as steel, alimentary, medical, and automotive [1,2]. This treatment consists of heating and cooling cycles, in which heat transfer methods such as radiation and convection are preferred because of its easy control schemes and implementation. The induction, microwave, and ohmic heating are more efficient but complex alternative methods [3,4], and besides, the ohmic heating is receiving particular attention due to its vast advantages like high-energy saving levels (82–97%), heating time reduction up to 90–95%, and high efficiency close to 100% [4].

As a consequence of a wide range of temperature capabilities, heating rates, and pattern reproducibility, this method is common in laboratory systems to study the microstructural effect [5–7], to perform research on steel phase transformation, and to conduct thermomechanical experiments [6]. In order to achieve this temperature performance, a control stage is imperative, and thus, a suitable model is crucial to determine the system's optimal control settings.

Models can be studied by multiphysics simulations using finite element methods [6]. Similarly, the computational fluid dynamics can generate detailed predictions of thermal profiles when fluids are involved [8]. On the other hand, a first approach model can be used to estimate its parameters using the experimental data [9], by using parameter estimation or optimization [10–12]. However, models are used during control tuning and stability stages, and then, simplified models are preferred for implementation.

The thermal circuit method is a tool that allows representing the heating performance of a system by using a simple electrical circuit [13], and even more, its transfer function allows to study both, steady and transient states, stability and control performance. Thus, the circuit allows to study how the system and the control will response under new control conditions, configuration, and system's parameters.

In this paper, an electrical circuit to model the temperature performance of an ohmic heating system is presented. The system was built to study microstructural effects on steel. The model is based on an energy balance and lumped-heat-capacity assumption, and no temperature gradient is considered. R and C parameters of the circuit are estimated using MATLAB scripts considering the mechanical, thermal, and electrical properties of the ohmic heating system. The circuit is solved by applying the Laplace transformation. The resulting data compare the model and experimental performance to validate the circuit method. Finally, the ohmic system together

Contributed by the Heat Transfer Division of ASME for publication in the JOURNAL OF THERMAL SCIENCE AND ENGINEERING APPLICATIONS. Manuscript received May 10, 2018; final manuscript received May 22, 2019; published online May 30, 2019. Assoc. Editor: Ayyoub M. Momen.

with the control scheme shows the accuracy performance during a thermal process.

2 Material and Methods

2.1 Experimental System. The modeled ohmic heating system is shown in Fig. 1. The aim of the system is to heat-up, maintain, and cool-down a hollow cylinder made up of 304 stainless steel, and this cylinder is labeled as *plant* in Fig. 1. The plant is heated by Joule effect using a direct current power supply (`Sorensen XFR7.5-300`), and this power supply can deliver up to 2800 W. A reflow subsystem is implemented to generate a specific hot zone on the plant, as reported in Ref. [14], and the subsystem reflows water through the inner cavity of the electrodes (see Fig. 2). The system also includes an argon gas based cooling subsystem to control the temperature sink rate over the sample; this gas subsystem uses an on-off controlled valve. Each actuator (dashed line in Fig. 1) is controlled by a cRio DAQ system. The temperature is measured through an exposed thermocouple directly welded in the plant to obtain a faster temperature response [15]; the measurements are also logged by the DAQ system.In Fig. 2, the ohmic heating elements are shown. Figure 2(*a*) shows a two-piece electrode, the gas inlet, and the inner cavity. Figure 2(*b*) shows the cylinder sample, and notice that the cylinder is mounted next to the gas inlet. Figure 2(*c*) shows the complete ohmic system assembled, and notice the four hose-holders to cool-down the electrodes by the water reflow system.

2.2 Thermal Model. The ohmic heating phenomenon, also known as direct heating, is an electrical heating method to produce a positive temperature variation due to the electrical power [4] defined by Eq. (1):

$$P(t) = V(t) \cdot I(t) = \frac{V^2(t)}{R_e} = I^2(t) \cdot R_e \tag{1}$$

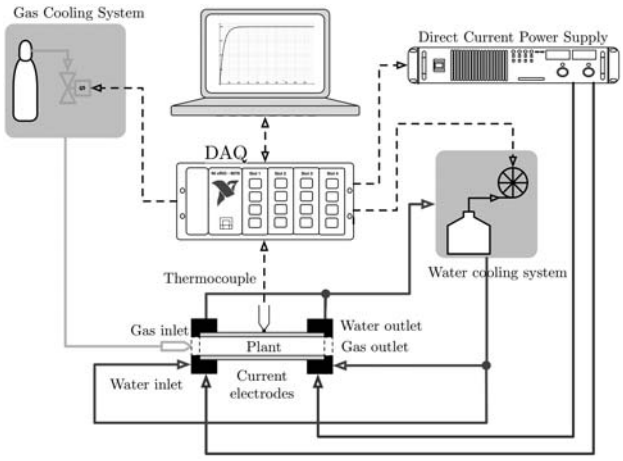

Fig. 1 Ohmic heating system setup: plant, gas cooling system, water cooling system, direct current power supply, and DAQ system

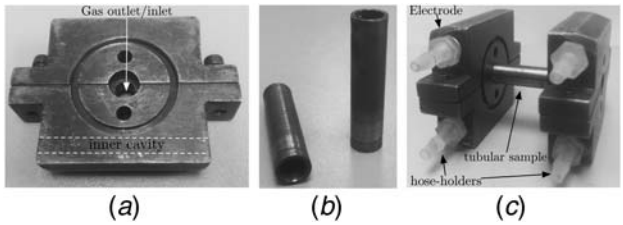

Fig. 2 Images of the plant: (*a*) an electrode to feed the current, gas, and water, (*b*) the tubular samples, and (c) the assembled plant

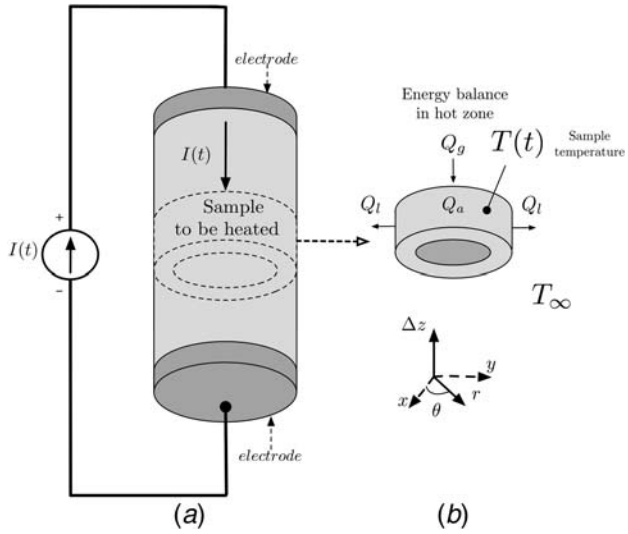

Fig. 3 Schematic of ohmic heating system: (*a*) simple scheme of the heating system and (*b*) section of the sample for the energy balance (*T*(*t*) is the sample temperature and T_∞ is the free stream temperature)

This method uses the material's electrical resistivity R_e to produce a voltage drop $V(t)$, due to a circulating current $I(t)$.

To define the thermal model for the ohmic heating system described in Eq. (1), a simplified schematic from the plant is presented in Fig. 3. This schematic shows two electrodes that feed the current $I(t)$ into the hollow cylinder. Then, by studying the isothermal zone [14] denoted by the volume element Δz and applying an energy balance at this point, Eq. (2) is derived:

$$\cancelto{0}{Q_i(t)} + Q_g(t) = Q_a(t) + Q_l(t) \tag{2}$$

This balance considers the generation $Q_g(t)$, the accumulation $Q_a(t)$, and the losing $Q_l(t)$ terms. However, the input $Q_i(t)$ is zero due to no extra heat is introduced.

2.2.1 Q_g, Q_a, and Q_l Terms. The generation term $Q_g(t)$ is function of the applied current and the cylinder's electrical resistance R_e:

$$Q_g(t) = I^2(t) \cdot R_e \tag{3}$$

where the R_e coefficient is the cylinder's electrical resistivity:

$$R_e = \frac{\rho_e \Delta z}{A_c} \tag{4}$$

where ρ_e is the cylinder's electrical resistivity, A_c is its cross-sectional area , and Δz is the length of the cylinder.

The accumulation term $Q_a(t)$ is defined in Eq. (5):

$$Q_a(t) = \rho C_p V \frac{dT(t)}{dt} \tag{5}$$

where ρ is the material's density, C_p is the material's specific heat, and V is the cylinder's volume.

Finally, the losing term $Q_l(t)$ is defined in Eq. (6):

$$Q_l(t) = A_s h_\tau [T(t) - T_\infty] \tag{6}$$

where A_s is the cylinder's superficial area, h_τ is the system's heat transfer coefficient, and T and T_∞ are the sample and free stream temperatures, respectively. All the coefficients involved in Eqs. (3)–(6) are detailed in Table 1.

Table 1 Electrical and thermal properties involved in Eqs. (3)–(6)

Parameter	Description	Units
$I(t)$	Circulating current	A
R_e	Electrical resistance	Ω
ρ_e	Electrical resistivity	Ω · m
Δz	Length of the sample	m
A_c	Cross-sectional area	m
C_p	Specific heat	W m^{-1} °C
ρ	Material's density	kg m^{-3}
A_s	Superficial area	m
h_τ	Heat transfer coefficient	W^2 m^{-1} °C
T_∞	Free stream temperature	°C
$T(t)$	Sample temperature	°C

Considering previous equations, Eq. (2) can be rewritten as Eq. (7):

$$I^2(t) \cdot \frac{\rho_e \Delta z}{A_c} = \rho C_p V \frac{dT(t)}{dt} + A_s h_\tau [T(t) - T_\infty] \tag{7}$$

With Eq. (7), it is possible to draw a circuit that represents the same differential equation.

2.3 Electrical Circuit Method. The electrical circuit method is used to represent thermal dynamics by using equivalent electrical systems [13]. Once the circuit is defined, it can be solved by several methods such as numerical methods [16], system identification [17], or neural networks [18]. This method is selected considering its complexity and application.

In this case, the ohmic heating system is modeled based on Eq. (7), and each one of the three terms involved is replaced by an electrical component. The left-hand term is considered as an energy input and modeled as a current source. The right-hand terms are modeled as a resistance R_{hs} and a capacitance C_{hs}. The differential term in function of the temperature is modeled as a capacitance. The voltage in the circuit is related to the temperature in the ohmic heating system. Thus, the linear term is modeled as a resistance device.

The equivalent electrical circuit is shown in Fig. 4. In the circuit, the current is analogous to the energy and the voltage to the temperature.

Considering the circuit and applying the Kirchhoff's current law at the A node, Eq. (8) is obtained:

$$Q_g(t) = Q_a(t) + Q_l(t) \tag{8}$$

However, currents Q_g, Q_a, and Q_l are rewritten considering the nodal voltages $T(t)$ and T_∞[1]:

$$Q_g(t) = C_{hs} \frac{d[T(t) - T_\infty]}{dt} + \frac{T(t) - T_\infty}{R_{hs}} \tag{9}$$

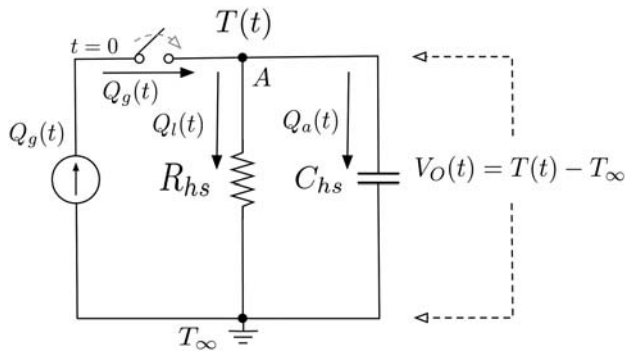

Fig. 4 Electrical model equivalent to the ohmic heating system

[1]Consider that T_∞ is a constant value that will disappear from the derivative term.

Table 2 Electrical and thermal terms equivalence

Thermal domain	Electrical domain	Term
$I^2(t) \cdot \frac{\rho_e \Delta z}{A_c}$	$Q_g(t)$	Generation
$\rho C_p V$	C_{hs}	Accumulation
$A_s h_\tau$	$1/R_{hs}$	Losses

where R_{hs} is the electrical resistance and C_{hs} is the electrical capacitance.

Note that Eqs. (7) and (9) have similar terms and are compared with estimate C_{hs} and R_{hs} values as a function of the geometry, electrical, and thermal properties of the sample. The terms comparison is shown in Table 2.

2.4 Transfer Function. A transfer function of a system links a variable response to an excitation signal. Several mathematical tools allow obtaining this transfer function, for instance, the Laplace transform. The transfer function is manipulated for a better understanding of the system's response and to design the controller for the system.

The Laplace transform was applied to Eq. (9) to relate the required energy input Q_g and the sample temperature T. Thus, Eq. (10) is obtained.

$$Q_g(s) = \frac{T(s) - T_\infty}{R_{hs}} + C_{hs}[sT(s) - T_0] \tag{10}$$

Solving for $T(s)$:

$$Q_g(s) = \frac{T(s)}{R_{hs}} - \frac{T_\infty}{R_{hs}} + sC_{hs}T(s) - C_{hs}T(0)$$

$$Q_g(s) = T(s)\left[\frac{1}{R_{hs}} + sC_{hs}\right] - \underbrace{\left[C_{hs}T(0) + \frac{T_\infty}{R_{hs}}\right]}_{T_c}$$

$$T(s)\left[\frac{1}{R_{hs}} + sC_{hs}\right] = Q_g(s) + T_c \tag{11}$$

$$T(s)\left[\frac{1 + sR_{hs}C_{hs}}{R_{hs}}\right] = Q_g(s) + T_c$$

$$T(s) = [Q_g(s) + T_c]\left[\frac{R_{hs}}{1 + sR_{hs}C_{hs}}\right]$$

In Eq. (11), considering T_c as a term that involves the initial temperature of the sample $T(0)$ and the free stream temperature T_∞, the transfer function $H(s)$ can be defined as follows:

$$H(s) = \frac{T(s)}{Q_g(s) + T_c} = \frac{R_{hs}}{1 + sR_{hs}C_{hs}}$$

Finally, the product $R_{hs}C_{hs}$ is defined as τ, then Eq. (12) is obtained.

$$H(s) = \frac{R_{hs}}{1 + s\tau} \tag{12}$$

3 Model Implementation

An script written in MATLAB was used to simulate the temperature response $T(t)$ of the ohmic heating system. The algorithm uses the function presented in Eq. (11). In this study, the parameters R_{hs} and C_{hs} were approximated by the equivalences shown in Table 2.

3.1 Parameters Calculation. The parameters calculation considers the geometry shown in Fig. 5. The value of C_{hs} was calculated using Eq. (13):

$$C_{hs} = \rho C_p V \tag{13}$$

where $V = A_b \times L$ in cubic meters, the A_b value is calculated by $A_b = \pi(r_e^2 - r_i^2)$ in square meters, the density value is consider as

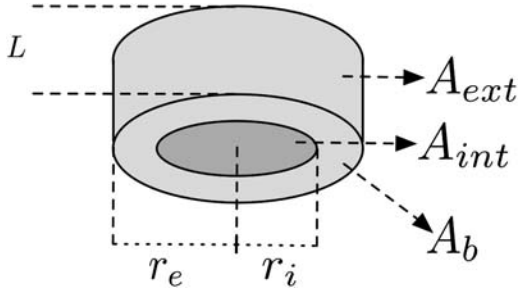

Fig. 5 Geometry of the hollow cylinder sample

$\rho = 8{,}024.3$ (kg m^3) for 304 stainless steel and a specific heat value $C_p = 502.32$ in (J/kg C). Listing 1 shows the calculation of C_{hs}.

Listing 1 Calculation of parameter C_{hs}

```
%Chs calculation :
%Chs= rho* Cp* V
length = 0.030;% Delta Z
extarnalRadius = 0.007/2; % 3.5mm
internalRadius = 0.005/2; % 2.5mm
baseArea = 3.141592* (extarnalRadius ^2 -
 internalRadius ^2);% Area from base
volume = baseArea* length;% m^3
density = 8024.3; % rho 304 density (Kg* m^3)
specificHeat = 502.32;%Cp 304 (J/KgC)
Chs = volume* density* specificHeat
```

The R_{hs} parameter was defined by Eq. (14).

$$R_{hs} = \frac{1}{A_s h_\tau} \tag{14}$$

where A_s is the total surface area calculated by Eq. (15). The terms involved in Eq. (15) are defined in Eqs. (16)–(18). The value of the heat transfer coefficient h_τ was estimated by the experimental procedures reported in Refs. [14,15]. For this model, the value of h_τ was considered as a constant function of the final value of the temperature. However, the average value of h_τ was clearly dominated by the radiation and conduction. The calculation of R_{hs} is shown in Listing 2.

$$A_s = A_{ext} + A_{int} + 2A_b \tag{15}$$

$$A_{ext} = 2\pi r_e L \tag{16}$$

$$A_{int} = 2\pi r_i L \tag{17}$$

$$A_b = \pi(r_e^2 - r_i^2) \tag{18}$$

Listing 2 Calculation of parameter R_{hs}

```
%Rhs calculation :
exteriorLateralArea = 2* 3.141592*
 extarnalRadius* length;
interiorLateralArea = 2* 3.141592*
 internalRadius* length;
areaTopBottom = 2* baseArea;
totalArea = exteriorLateralArea +
 interiorLateralArea + areaTopBottom;
heatTransferCoefficient = 120;
Rhs=1/(totalArea* heatTransferCoefficient);
```

Then, to model the system's temperature response against time, $Q_g(s)$ and T_c terms from Eq. (11) must be defined. Q_g is the energy input and T_c is the system's condition. Their implementation and calculation are shown in Listing 3.

Listing 3 Calculation of Q_a and T_c terms

```
%Tc term calculation :
T0=27; %celsius
Tinf=27; %celsius
Tc=Chs* T0/tFinal+Tinf/Rhs;
%Generation term calculation
electricalResistivity = 0.00000116;
Re = length* electricalResistivity/baseArea
Iin1=150;, Iin2=190;, Iin3=230;, Iin4=240;
Qg1 = Iin1* Iin1* Re;
Qg2 = Iin2* Iin2* Re;
Qg3 = Iin3* Iin3* Re;
Qg4 = Iin4* Iin4* Re;
```

Notice that the T_c term is divided by `tFinal` to transform Joules to Watts; this variable is the total time of the simulation. In line 9, four current values are used to calculate the Q_g input terms.

3.2 System's Response to the Step Input. The system's response is calculated using the code shown in Listing 4. The resulting plots are shown in Fig 6. The figure shows the inverse Laplace transformation of the function `ohTFs`, and the function is forced by the scale step input $(Qgx + Tc)/s$, with $Qg1$, $Qg2$, $Qg3$, and $Qg4$. Each Qg value was calculated considering the input current values.

Listing 4 Step system's response

```
%Plotting data for external post-processing
syms s t;
ohTFs=Rhs./(Rhs.* Chs* s+1);
t=0:1:tFinal;
%Step responses :
oht1=ilaplace((Qg1+Tc)/s* ohTFs,s,t);
oht2=ilaplace((Qg2+Tc)/s* ohTFs,s,t);
oht3=ilaplace((Qg3+Tc)/s* ohTFs,s,t);
oht4=ilaplace((Qg4+Tc)/s* ohTFs,s,t);
plot(t,oht1,t,oht2,t,oht3,t,oht4)
```

4 Results and Discussion

In order to validate the model, a series of no controlled experiments were performed. In each experiment, fixed values of current were fed into the system. The temperature data were recorded by the DAQ system through the thermocouple. The obtained data were postprocessed to compensate the offset value, and the resulting data were compared with the model's performance. Finally, the complete ohmic system is tested along with its controller.

4.1 Open-Loop Experiments. The open-loop or noncontrolled experiments implementation is shown in Fig. 7. A fixed current value was programmed on the power supply and then fed into the ohmic system represented by its model equation. The current value is modified by the control voltage $V_c(t)$, and the output temperature $T(t)$ was recorded by the DAQ system through the thermocouple.

Figure 8 depicts the measurements temperature during each noncontrolled experiment. Thus, the input currents were constant signals with values of 150, 190, 230, and 240 A. The current was

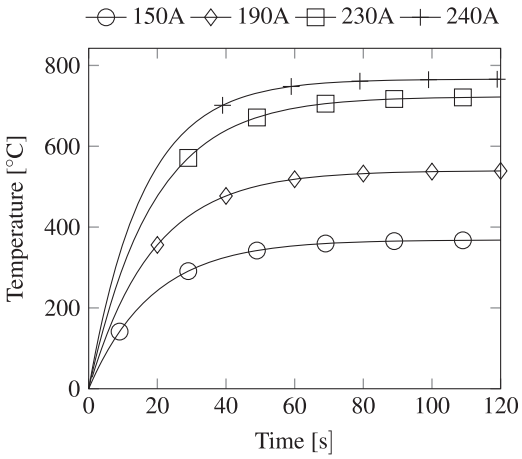

Fig. 6 Transfer function's temperature response for constant input currents: 150 A, 190 A, 230 A, and 150 A

fed between $t = 10$ s and $t = 120$ s. The cooling for the experiments was done by natural convection and the electrodes cooling system.

Note that in $t = 10$ s, a sudden change (dotted circle) takes place due to the circulating current through the thermocouple's joint [15]. This offset value was eliminated during the postprocess stage by subtraction. Also note that the thermal response shows a stable behavior under low current values (150 A and 190 A). This can be attributed to the material's electrical resistivity variations at high temperatures and the formation of thin films of oxide.

4.2 Model and Experimental Comparison. To compare the model and the experimental system, both data are plotted as shown in Figs. 9 and 10. Figure 9 shows the thermal response for $I = 150$ A and $I = 240$ A. Meanwhile, Fig. 10 shows the response for $I = 190$ A and $I = 230$ A.

The electrical circuit model has a proper response for all current values. However, the experimental system rises slightly faster than the model. This difference could be associated with the use of h_τ as a constant value instead of a linear or polynomial function approximation.

Specifically, the h_τ value was determined as a compound factor of the water cooling system and system's convection. Thus, the fluctuations in the steady-state region can be linked to air bubbles in the hose, small variations in the speed of the pump, changes in the electrical resistance due to the temperature, or the grow of thin skin of oxide; all these factors can modify momentarily the value of the current fed into the system.

4.3 Tuning and Controlled Experiments. Figure 11 shows the close-loop or controlled experiments setup. Here, $r(t)$ is the reference temperature programmed in the computer, and $y(t)$ is the temperature measurement done by the thermocouple. The

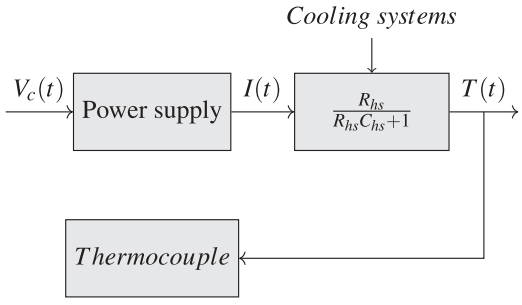

Fig. 7 Noncontrolled experiments implementation

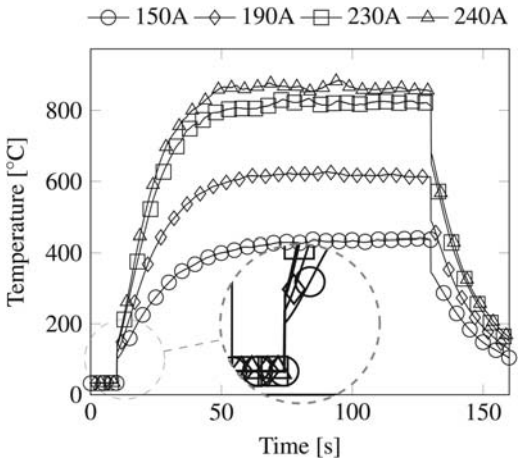

Fig. 8 Thermal response of ohmic heating system

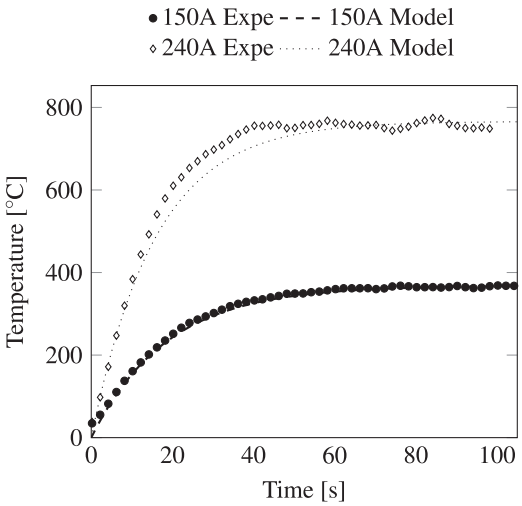

Fig. 9 Thermal response of the electrical circuit model and open-loop experiments for $I = 150$ A and $I = 240$ A

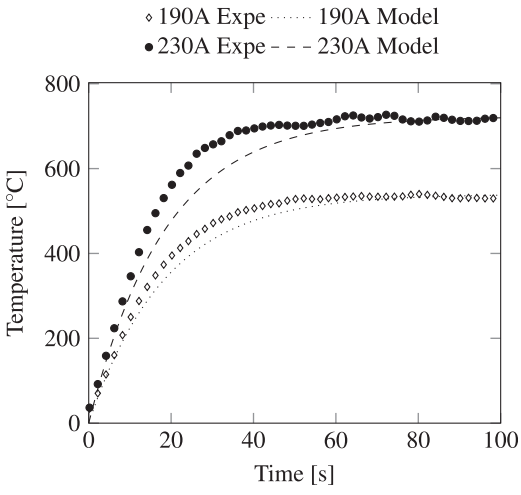

Fig. 10 Thermal response of the electrical circuit model and open-loop experiments for $I = 190$ A and $I = 230$ A

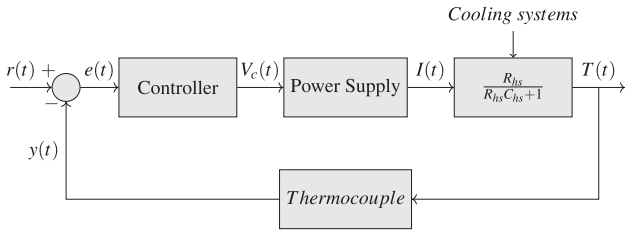

Fig. 11 Controlled experiment setup

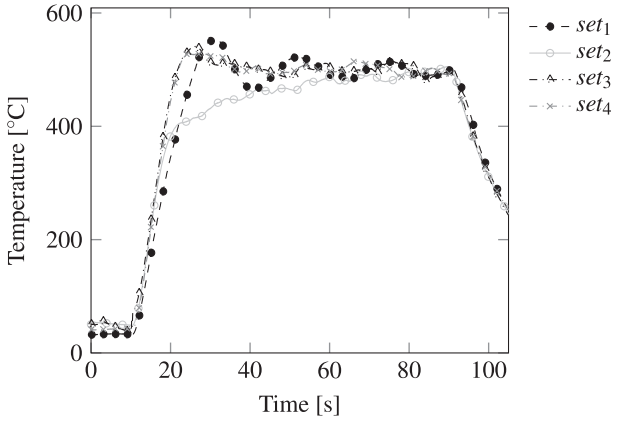

Fig. 12 Thermal response of the ohmic system to the set of values during the tuning process

difference between $r(t)$ and $y(t)$ is known as the error $e(t)$. This signal is used to tune the controller performance of the power supply.

4.3.1 Tuning Experiments. In Fig. 12, the system's tuning process is shown. This process is normally done manually. Thus, the tuning values are selected considering how fast/slow the system must react. The figure shows a set of four gains on the controller. The set_1 has a medium heating rate with an oscillating behavior to reach the programmed temperature value: 500 °C. The control's oscillating performance is called "underdamped control." On the other hand, set_2 has a more slow heating rate or "overdamped control."

4.3.2 Controlled Experiments. After adjusting the controller's gains, the system is ready to perform controlled experiments. Figure 13 shows two experiments, both to maintain 800 °C for 90 s and then to force to cool-down the sample, first without gas pressure 0 psi and the second experiment with 180 psi. Note

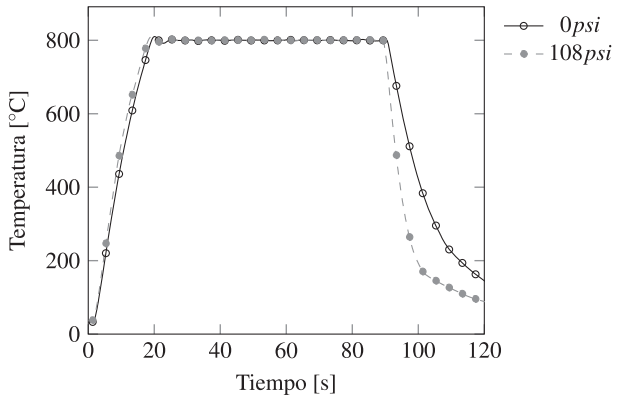

Fig. 13 Heating system performance with controller

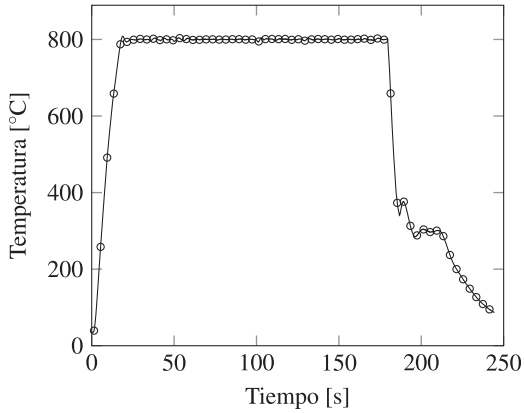

Fig. 14 Heating system performance for two-level experiment

Table 3 Ohmic system performance with controller

		Heating stage		Cooling stage	
No. of test	T_1 (°C)	Heating rate (°C s^{-1})	Rise time (s)	Pressure (psi)	Cooling rate (°C s^{-1})
P_1	800	44.96	13.71	0	−35.41
P_2	900	46.52	15.5	0	−37.86
P_3	800	46.11	12.91	40	−47.83
P_4	800	45.47	13.31	40	−51.46
P_5	800	46.36	12.81	108	−75.4
P_6	800	46.3	12.75	108	−81.87
P_7	900	49.03	14.196	108	−85.76

that experiments reach fast and smoothly the temperature's final value, and also minimal variations are presented along the experiment.Another experiment is shown in Fig. 14. Here, a first temperature value was set to 800 °C and maintained during 180 s. Then, a new temperature value was set to 300 °C and forced to cooling by pressured gas at 180 psi during 5 s. Note that the controller has an overshot to compensate the temperature changes, temperature was maintained during 20 s, and then the controller stops to feed current.

Table 3 shows a series of seven additional experiments to obtain heating and cooling rates. These data were obtained from heating and cooling stages. The heating rate column shows that the system and its controller allow maximum rates of 49 °C s^{-1} and minimum of 45 °C s^{-1}. Also, the data allow to know the nominal rise time of the system: a maximum of 15 s. For the cooling stage, note that the system by natural convection process has a maximum of 37 °C s^{-1} and a maximum of 85 °C s^{-1} by forced convection at 108 psi.

5 Conclusion

The obtained model was based on a basic RC circuit analogy that represents adequately the ohmic heating system dynamics. The model includes the input energy as a current source. This input was calculated considering the electrical resistance of the sample and its geometry. The parameters are defined by the volume, areas, and electromechanical properties of the system. However, the accuracy of the circuit is limited to estimate previously the h_τ value. Also, the model only gives a single point temperature value, and temperature distribution is not reliable. Nevertheless, the basic system dynamics is well predicted. Considering that the final application of the model is to estimate the required current, as well as the dynamic and steady-state performances of the heating system through the R and C parameters, the model is functional and relates adequately the output temperature to the system definition.

Even more, the model allows to study and simulate the system to design the temperature controller, to analyze its stability, and to determine how the material and its geometry will affect the system to reach the required temperature, establishing the needs of electric power. The controller allows to reach maximum heating rates of 49 °C s^{-1} and sinking rates of −85 °C s^{-1}.

More complex models can be developed using the circuit method by sectioning the whole piece in several segments, imitating the finite element method, and proposing more boundary conditions to include the convective and conductive effects as separated terms.

Acknowledgment

The authors would like to thank to the National Laboratory "SEDEAM" at Morelia city, Mexico, for all the support given to this research and the use of equipment acquired through the project Nos. 235780, 271878, and 282357.

References

[1] Peng, Y.-C., Jin, H.-J., Liu, J.-H., and Li, G.-L., 2012, "Influence of Cooling Rate on the Microstructure and Properties of a New Wear Resistant Carbidic Austempered Ductile Iron (cadi)," Mater. Charact., **72**, pp. 53–58.

[2] Deak, T., and Lelieveld, Y. M., 2014, "Chapter 17—Thermal Treatment," *Food Safety Management: A Practical Guide for the Food Industry*, Academic Press, San Diego, CA, pp. 423–442.

[3] Knirsch, M. C., Alves dos Santos, C., Martins de Oliveira Soares Vicente, A. A., and Vessoni Penna, T. C., 2010, "Ohmic Heating—A Review," Trends Food. Sci. Technol., **21**(9), pp. 436–441.

[4] Sakr, M., and Liu, S., 2014, "A Comprehensive Review on Applications of Ohmic Heating (OH)," Renewable Sustainable Energy. Rev., **39**, pp. 262–269.

[5] Fabrègue, D., Mouawad, B., and Hutchinson, C. R., 2014, "Enhanced Recovery and Recrystallization of Metals Due to An Applied Current," Scr. Mater., **92**(92), pp. 3–6.

[6] Kim, H. Y., Park, J. K., and Lee, M.-G., 2014, "Phase Transformation-Based Finite Element Modeling to Predict Strength and Deformation of Press-Hardened Tubular Automotive Part," Int. J. Adv. Manuf. Technol., **70**(9), pp. 1787–1801.

[7] Sarkis, J. R., Mercali, G. D., Tessaro, I. C., and Marczak, L. D. F., 2013, "Evaluation of Key Parameters During Construction and Operation of An Ohmic Heating Apparatus," Innov. Food Sci. Emerg. Technol., **18**, pp. 145–154.

[8] Varghese, K. S., Pandey, M. C., Radhakrishna, K., and Bawa, A. S., 2012, "Technology, Applications and Modelling of Ohmic Heating: A Review," J. Food Sci. Technol., **51**(10), pp. 2304–2317.

[9] Feng, K., Ying, Z., and Tong, X., 2015, "Radial Thermal Circuit Model for Overhead Conductors Based on Parameter Identification Under Natural Convection Condition," 2015 IEEE Power & Energy Society General Meeting, Denver, CO, July 26–30, pp. 0–4.

[10] Chen, Q., Fu, R.-H., and Xu, Y.-C., 2015, "Electrical Circuit Analogy for Heat Transfer Analysis and Optimization in Heat Exchanger Networks," Appl. Energy, **139**, pp. 81–92.

[11] Zhao, S. Y., and Chen, Q., 2016, "A Thermal Circuit Method for Analysis and Optimization of Heat Exchangers With Consideration of Fluid Property Variation," Int. J. Heat Mass Transf., **99**, pp. 209–218.

[12] Chen, Q., Hao, J. H., and Zhao, T., 2017, "An Alternative Energy Flow Model for Analysis and Optimization of Heat Transfer Systems," Int. J. Heat Mass Transf., **108**, pp. 712–720.

[13] Preissler, S., Goncalves, A. L., and Fernandes, W. R., 2016, "A Framework for Multi-Zone Building Thermal-Electrical Representation," 2016 12th International Conference on Intelligent Environments (IE), London, UK, Sept. 14–16, pp. 167–170.

[14] Herrejón-Escutia, M., Solorio-Díaz, G., Vergara-Hernández, H., López-Martínez, E., Chávez-Campos, G., and Vázquez-Gómez, O., 2017, "Electric-Thermo-Mechanical Analysis of Joule Heating in Dilatometric Specimens," Stroj. Vestnik/J. Mech. Eng., **63**(9), pp. 537–547.

[15] Chávez-Campos, N. P., Chávez-Campos, G. M., and SalazarTorres, J. A., 2015, "Fast Response Temperature Model Based on Thermal Data for Joule Heating Process Using Exposed Joint Thermocouple Method," 2015 IEEE International Autumn Meeting on Power, Electronics and Computing (ROPEC), Ixtapa, Mexico, Nov. 4–6, pp. 1–4.

[16] Preissler, S., 2016, "A Framework for Thermal Parameter Identification in a Smart Buildings Context," 2016 IEEE International Smart Cities Conference (ISC2), pp. 8–11.

[17] Glotic, A., 2016, "Identification of Thermal Parameters for Transformer FEM Model by Differential Evolution Optimization Algorithm," 2016 International Conference Multidisciplinary Engineering Design Optimization (MEDO), pp. 1–6.

[18] Jambunathan, K., Hartle, S. L., Ashforth-Frost, S., and Fontama, V. N., 1996, "Evaluating Convective Heat Transfer Coefficients Using Neural Networks," Int. J. Heat. Mass. Transfer, **39**(11), pp. 2329–2332.